haematologica
Journal of The Ferrata Storti Foundation

Daratumumab inhibits acute myeloid leukaemia metabolic capacity by blocking mitochondrial transfer from mesenchymal stromal cells

by Jayna J Mistry, Jamie A Moore, Prakritt Kumar, Christopher R Marlein, Charlotte Hellmich, Genevra Pillinger, Aisha Jibril, Federica Di Palma, Angela Collins, Kristian M Bowles, and Stuart A. Rushworth

Haematologica 2020 [Epub ahead of print]

Citation: Jayna J Mistry, Jamie A Moore, Prakritt Kumar, Christopher R Marlein, Charlotte Hellmich, Genevra Pillinger, Aisha Jibril, Federica Di Palma, Angela Collins, Kristian M Bowles, and Stuart A. Rushworth. Daratumumab inhibits acute myeloid leukaemia metabolic capacity by blocking mitochondrial transfer from mesenchymal stromal cells.
Haematologica. 2020; 105:xxx
doi:10.3324/haematol.2019.242974

Daratumumab inhibits acute myeloid leukaemia metabolic capacity by blocking mitochondrial transfer from mesenchymal stromal cells

Jayna J Mistry[1,2], Jamie A Moore[1], Prakritt Kumar[1], Christopher R Marlein[1], Charlotte Hellmich[1,3], Genevra Pillinger[1], Aisha Jibril[1], Federica Di Palma[1,2], Angela Collins[3], Kristian M Bowles[1,3]** and Stuart A Rushworth[1]**

[1] Norwich Medical School, University of East Anglia, Norwich Research Park, Norwich, NR4 7UQ, United Kingdom.
[2] Earlham Institute, Norwich Research Park, Norwich, NR4 7UH, United Kingdom
[3] Department of Haematology, Norfolk and Norwich University Hospitals NHS Trust, Colney Lane, Norwich, NR4 7UY, United Kingdom

**Denotes joint corresponding author
Running Title: Daratumamab inhibits mitochondrial transfer to AML

Corresponding authors: Dr Stuart Rushworth and Prof Kristian Bowles, Department of Molecular Haematology, Norwich Medical School, Norwich Research Park, Norwich, NR4 7UQ, United Kingdom. email: s.rushworth@uea.ac.uk and k.bowles@uea.ac.uk

Acute Myeloid Leukaemia [AML] proliferation is dependent on a complex multi-faceted interplay between the blasts and the bone marrow microenvironment (1). We and others have previously demonstrated that functional mitochondria are transferred from the MSC to the AML blasts facilitating progression of the disease (2, 3), in a process which is hijacked from haematopoietic stem cell response to infection (4). Clinical observations trials using Venetoclax, which targets BCL2 (which in turn is a key regulator of the mitochondrial apoptotic pathway), in combination with hypomethylating agents showed tolerable safety and favorable overall response rate in elderly patients with AML (5). Taken together these data imply that mitochondria represent an attractive and biologically plausible drug target in the treatment of AML.

CD38 is a transmembrane glycoprotein which is expressed on many cells of the haematopoietic system including malignant plasma cells, red blood cells, myeloid cells, lymphoid cells and subsets of leukaemia initiating AML blasts (6-8). Furthermore we have recently shown that CD38 mediates pro-tumoral mitochondrial transfer from mesenchymal stromal cells (MSC) to malignant plasma cells in myeloma (9), which in part explains why Daratumumab (an anti-CD38 monoclonal antibody) is clinically effective in treating patients with myeloma (10). More recently, daratumumab has been shown to have preclinical activity in AML (11). Therefore, taken together we hypothesise that daratumumab treatment would impair AML metabolic capacity and consequently inhibit tumour proliferation, via a mechanism which blocks mitochondrial transfer from BMSC to the blasts.

Initially, to determine if CD38 inhibition blocks mitochondrial transfer from MSC to AML blasts, we used an in vitro co-culture system. MitoTracker Green FM stain was used to quantify mitochondria in AML after coculture with MSC. We incubated both MSC and AML with MitoTracker Green FM. The cells were washed twice in PBS and incubated for 4 h. The cells were then cocultured for 24 h with and without darartumumab. AML was shown to have less MitoTracker fluorescence when treated with daratumumab, using flow cytometry (Figure 1A-C). Figure 1D shows the presence of mouse mtDNA in human AML after co-culture with mouse MSC and the transfer of mouse mtDNA to human AML was inhibited by the addition of daratumumab. We further showed that knockdown of CD38 inhibited mitochondrial content in AML when cultured with MSC (figure1E and F). We next investigated if daratumumab could inhibit AML disease progression in vivo. To do this we used an NSG mouse model of AML whereby on day 1 we transplanted $0.5x10^6$ OCI-AML3 cells tagged with a luciferase construct into the tail vein of NSG mice (3), we then treated the NSG animals with either vehicle control (PBS) or daratumumab (5mg/kg) on day 9 and day 16 by intra-peritoneal (IP) injection (Figure 2A). The mice were then imaged using bioluminescence on day 21. Figure 2B shows bioluminescence from live in-vivo imaging. The pre-treatment tumor burden was the same between treatment and control animals on day 9, however following treatment with daratumumab the tumor burden in treated animals was significantly reduced when compared to mice in the vehicle control group. The densitometry measurement of these images are in figure 2C to illustrate the differences between vehicle and daratumumab treated animals. These data show that there was less tumor derived bioluminescence intensity in the daratumumab treated animals when compared to control. Daratumumab treated animals also had increased overall survival compared to controls animals (Figure 2D).

To determine how daratumumab altered the metabolic profile and function of the AML cells in vivo we again transplanted $0.5x10^6$ OCI-AML3-luc cells and treated the mice as described in Figure 2. The mice were then sacrificed on day 21 and OCI-AML3-luc cells were isolated by cell sorting from mouse bone marrow and the cells were analysed ex vivo (Figure 3A). The mitochondrial mass within the OCI-AML3-luc cells was not significantly reduced in the animals treated with daratumumab compared to the control animals (Figure 3B). Mitochondrial potential measured by Tetramethylrhodamine, Methyl Ester, Perchlorate (TMRM) staining shows that the OCI-AML3-luc cells had a reduced mitochondrial potential in the daratumumab treated animals compared to the control vehicle treated NSG mice (Figure 3C). To determine whether daratumumab altered mitochondrial based metabolism we analysed the OCI-AML3-luc cells isolated from the vehicle control and the daratumumab treated animals and then measured oxygen consumption rate (OCR) using the Seahorse Cell Mito Stress Test assay. Figure 3D shows decreased mitochondrial respiration was observed in the OCI-AML3-luc cells from daratumumab treated animals compared to OCI-AML3-luc cells from control treated mice. To investigate if mitochondrial transfer from the bone marrow microenvironment to the AML was altered with daratumumab treatment the human OCI-AML3-luc cells were isolated from murine bone marrow by cell sorting and analysed for the presence of mouse mitochondrial DNA within the human OCI-AML3-luc cells by TaqMan Real-time PCR. Figure 3E confirms that daratumumab treatment inhibited mouse mitochondrial DNA transfer to human OCI-AML3-luc cells. Together, these results reason, in vivo, that daratumumab treatment causes OCI-AML3-luc cells to have a decrease in AML mitochondrial mass, reduction of AML transfer from MSC to AML blasts and may contribute to the inhibitory functional bio-energetic consequence in AML metabolism in the bone marrow microenvironment.

In conclusion, CD38 inhibition results in reduced mitochondrial transfer from MSC to AML blasts in the BM microenvironment, resulting in a reduction in AML derived oxidative phosphorylation and subsequent reduced tumor burden. While it is likely that daratumumab functions through a number of mechanisms of action, here we show in an NSG mouse model lacking functional B cells, T cells and NK cells, that inhibition of mitochondrial transfer can be added to the list of mechanisms of action for this drug in AML. These data support the further investigation of daratumumab as a therapeutic approach for the treatment of mitochondrial dependent tumour growth.

Acknowledgements
The authors wish to thank the Norwich Medical School, the United Kingdom National Health Service, the Big C and the Rosetrees Trust for funding and the Norwich Biorepository (UK) for help with sample collection and storage. pCDH-Lucferase-T2A-mCherry was kindly gifted by Professor Irmela Jeremias, MD, from Helmholtz Zentrum München, Munich, Germany. The authors also thank Allyson Tyler, Dr Ian Thirkettle and Karen Ashurst from the Laboratory Medicine Department at the Norfolk and Norwich University Hospital for technical assistance.

Author Contribution
K.M.B and S.A.R designed the research; J.J.M., J.A.M., C.R.M., C.H., G.P., P.K., A.J., and S.A.R. performed the research; A.C., F.D.P., and K.M.B. provided essential reagents and knowledge. J.J.M., K.M.B., and S.A.R. wrote the paper.

Conflict of interests
K.M.B and S.A.R. received funding from Jannsen Pharmaceuticals for this study.

References

1. Shafat MS, Gnaneswaran B, Bowles KM, Rushworth SA. The bone marrow microenvironment - Home of the leukemic blasts. Blood Rev. 2017;31(5):277-286.
2. Moschoi R, Imbert V, Nebout M, et al. Protective mitochondrial transfer from bone marrow stromal cells to acute myeloid leukemic cells during chemotherapy. Blood. 2016;128(2):253-264.
3. Marlein CR, Zaitseva L, Piddock RE, et al. NADPH oxidase-2 derived superoxide drives mitochondrial transfer from bone marrow stromal cells to leukemic blasts. Blood. 2017;130(14):1649-1660.
4. Mistry JJ, Marlein CR, Moore JA, et al. ROS-mediated PI3K activation drives mitochondrial transfer from stromal cells to hematopoietic stem cells in response to infection. Proc Natl Acad Sci U S A. 2019;116(49):24610-24619.
5. DiNardo CD, Pratz K, Pullarkat V, et al. Venetoclax combined with decitabine or azacitidine in treatment-naive, elderly patients with acute myeloid leukemia. Blood. 2019;133(1):7-17.
6. Deaglio S, Mehta K, Malavasi F. Human CD38: a (r)evolutionary story of enzymes and receptors. Leuk Res. 2001;25(1):1-12.
7. Taussig DC, Vargaftig J, Miraki-Moud F, et al. Leukemia-initiating cells from some acute myeloid leukemia patients with mutated nucleophosmin reside in the CD34(-) fraction. Blood. 2010;115(10):1976-1984.
8. Sarry J-E, Murphy K, Perry R, et al. Human acute myelogenous leukemia stem cells are rare and heterogeneous when assayed in NOD/SCID/IL2Rγc-deficient mice. J Clin Invest. 2011;121(1):384-395.
9. Marlein CR, Piddock RE, Mistry JJ, et al. CD38-driven mitochondrial trafficking promotes bioenergetic plasticity in multiple myeloma. Cancer Res. 2019;79(9):2285-2297.
10. van de Donk NWCJ, Usmani SZ. CD38 Antibodies in Multiple Myeloma: Mechanisms of Action and Modes of Resistance. Front Immunol. 2018;9:2134.
11. Naik J, Themeli M, de Jong-Korlaar R, et al. CD38 as a therapeutic target for adult acute myeloid leukemia and T-cell acute lymphoblastic leukemia. Haematologica. 2019;104(3):e100-e103.

Figure legends

Figure 1. CD38 inhibition blocks mitochondrial transfer from MSC to AML blasts. (A) Primary AML and MSC were pre-stained with MitoTracker green FM for 1hour and then cultured alone or together for 24 hours. Flow cytometry was used to detect MitoTracker green FM in the AML blasts (n=8). (B) Primary AML and MSC were pre-stained with MitoTracker green FM for 1hour and then cultured together for 24hours in the presence of vehicle or daratumumab (100ng/ml). Flow cytometry was used to detect MitoTracker green FM in the AML blasts (n=6). (C) Primary AML were pre-stained with MitoTracker green FM for 1 hour and then treated with vehicle or daratumumab for 24 h (100ng/ml). Flow cytometry was used to detect MitoTracker green FM in the AML blasts (n=5). (D) Human AML was cultured with mouse MSC in the presence of vehicle or daratumumab for 24 h (100ng/ml) for 24 hours. AML were isolated and measured for mouse mitochondrial DNA content. Primary AML were transduced with CD38 targeted shRNA for 48 hours. (E) RNA was then extracted and examined for CD38 mRNA expression. (F) AML and MSC were then

pre-stained with MitoTracker green FM for 1hour and then cultured together for 24 hours. Flow cytometry was used to detect MitoTracker green FM in the AML blasts (n=4). We used the Mann-Whitney *U* test and Wilcoxon matched pairs signal rank test, to compare results between groups

Figure 2. Daratumumab inhibits AML disease progression in vivo. (A) Schematic of. the in-vivo model for these experiments. (B) $0.5x10^6$ OCI-AML3-luc cells were injected into the tail vein of NSG mice. Mice were imaged using bioluminescence at day 9 following injection to confirm tumor engraftment, and then split into two groups. Group 1 received vehicle (PBS) and group 2 received daratumumab (Dara; 5mg/kg) on day 9 and day 16 by intra-peritoneal (IP) injection. Mice were then imaged using bioluminescence at day 21 and then sacrificed. (C) Densitometry of the bioluminescent images shown in (B) was performed to determine differences between vehicle and daratumumab treated animals. (D) In a separate experiment, Kaplan-Meier survival curves for C57BL/6 (n=5) mice injected with $0.5x10^6$ OCI-AML3-luc and then treated with vehicle or daratumumab at day 9 and 16 post injection, was performed. We used the Mann-Whitney *U* test to compare results between groups. The Mantel-Cox test was used to analyse Kaplan-Meier survival curves.

Figure 3. Daratumumab alters the metabolic function of AML cells in vivo. (A) Schematic of the in-vivo model for these experiments. $0.5x10^6$ OCI-AML3-luc cells were injected into the tail vein of NSG mice. Mice were imaged using bioluminescence at day 9 following injection to confirm tumor engraftment, and then split into two groups. Group 1 received vehicle (PBS) and group 2 received daratumumab (Dara; 5mg/kg) treatment on day 9 and day 16 by intra-peritoneal (IP) injection. Mice were then sacrificed at day 21 and OCI-AML3-luc cells were isolated by cell sorting from mouse bone marrow and analysed for (B) Mitochondrial content by MitoTracker Green staining. (C) Mitochondrial potential by Tetramethylrhodamine, Methyl Ester, Perchlorate (TMRM) staining. (D) Oxygen consumption rate (OCR) by Seahorse Cell Mito Stress Test kit. (E) Presence of mouse mitochondrial DNA by Real-time PCR. We used the Mann-Whitney *U* test to compare results between groups

Figure 1

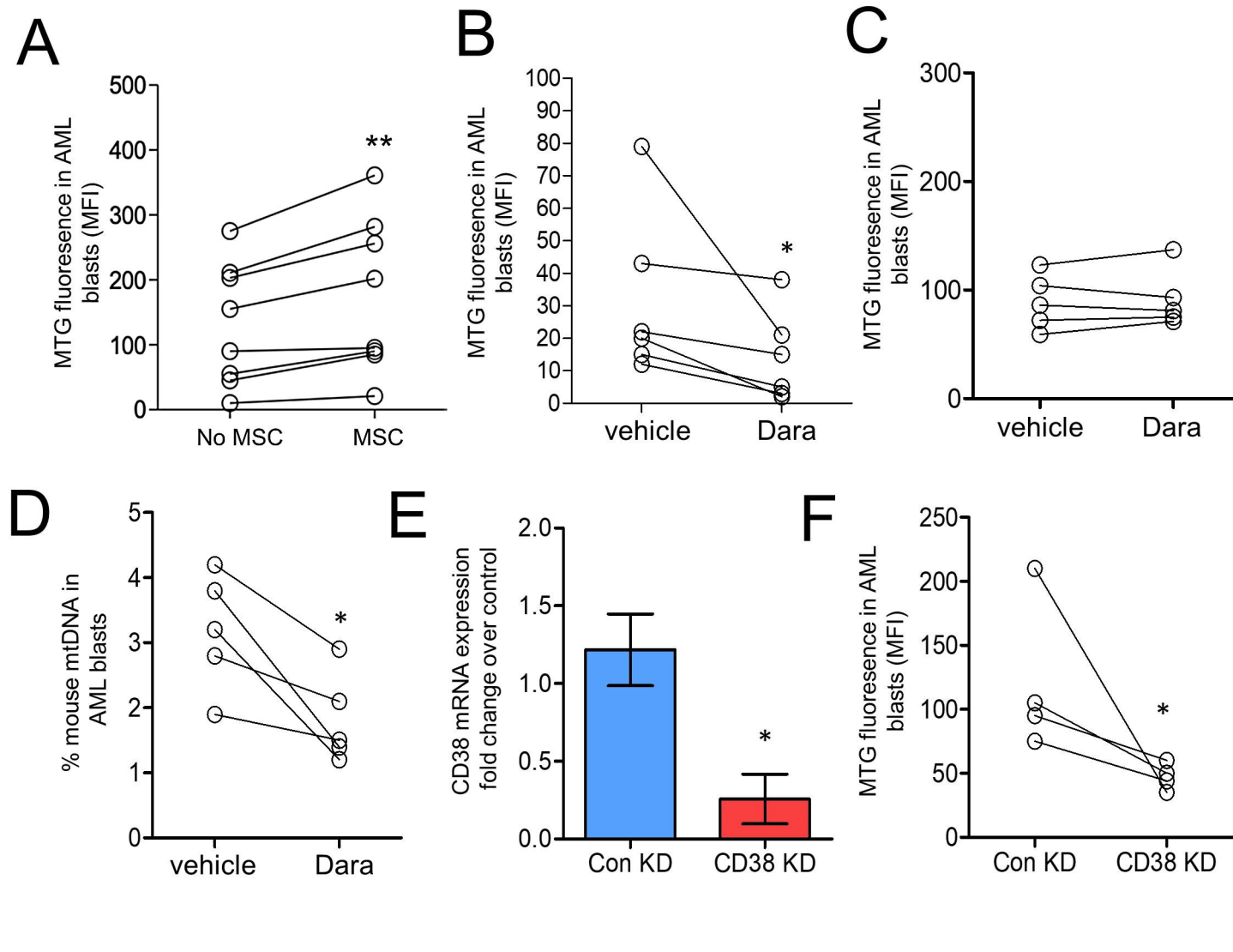
A
MTG fluoresence in AML blasts (MFI)
500
400
300
200
100
0
**
No MSC
MSC
B
MTG fluoresence in AML blasts (MFI)
100
90
80
70
60
50
40
30
20
10
0
*
vehicle
Dara
C
MTG fluoresence in AML blasts (MFI)
300
200
100
0
vehicle
Dara
D
% mouse mtDNA in AML blasts
5
4
3
2
1
0
*
vehicle
Dara
E
CD38 mRNA expression fold change over control
2.0
1.5
1.0
0.5
0.0
*
Con KD
CD38 KD
F
MTG fluoresence in AML blasts (MFI)
250
200
150
100
50
0
*
Con KD
CD38 KD

Figure 2

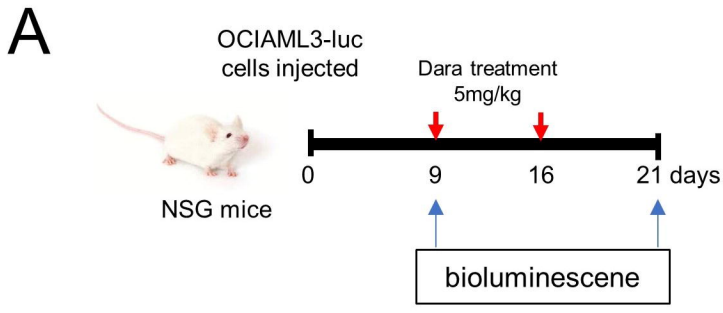
A
OCIAML3-luc
cells injected
Dara treatment
5mg/kg
NSG mice
0
9
16
21 days
bioluminescene

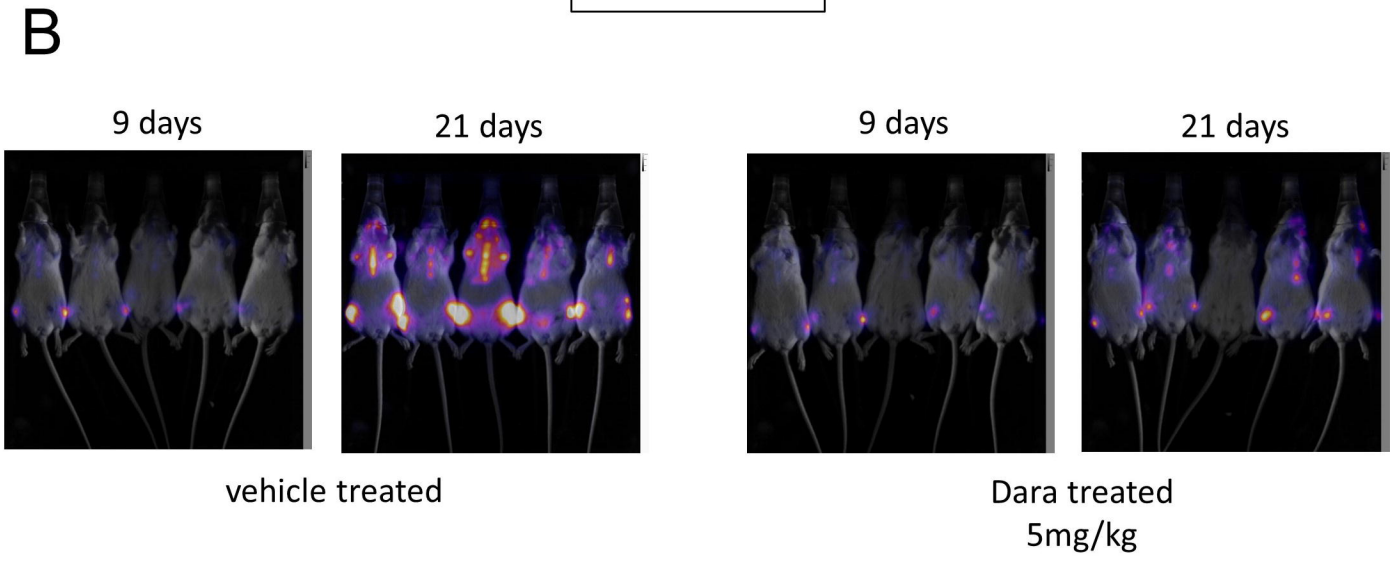
B
9 days
21 days
9 days
21 days
vehicle treated
Dara treated
5mg/kg

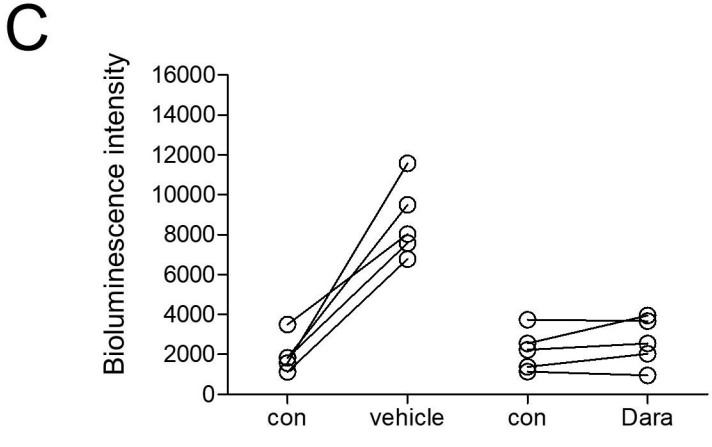
C
Bioluminescence intensity
16000
14000
12000
10000
8000
6000
4000
2000
0
con
vehicle
con
Dara

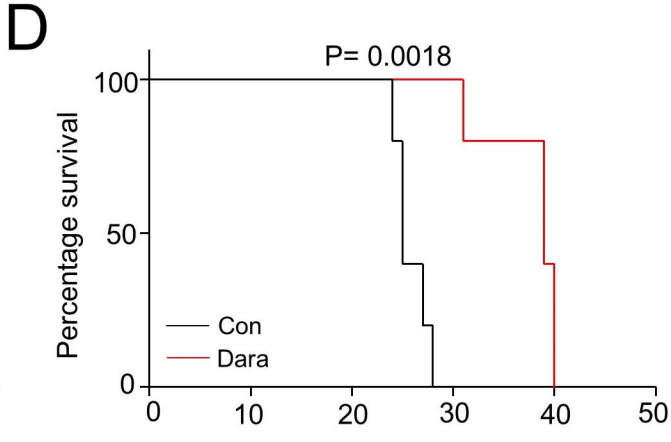
D
P= 0.0018
Percentage survival
100
50
0
Con
Dara
0
10
20
30
40
50

Figure 3

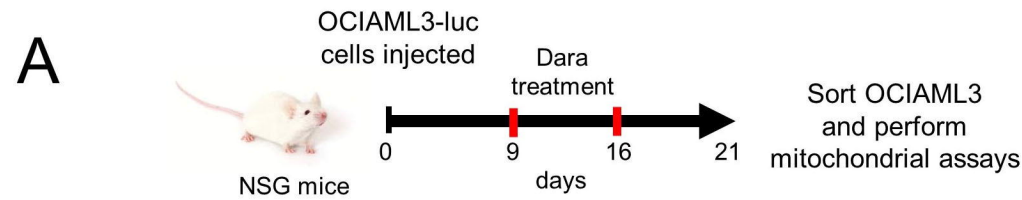
A
OCIAML3-luc
cells injected
Dara
treatment
NSG mice
0
9
16
21
days
Sort OCIAML3
and perform
mitochondrial assays

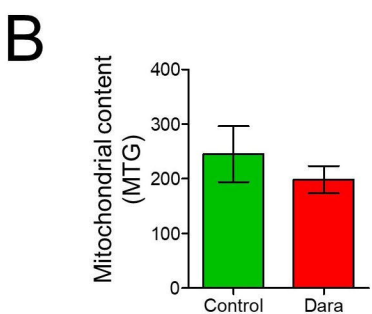
B
Mitochondrial content
(MTG)
400
300
200
100
0
Control
Dara

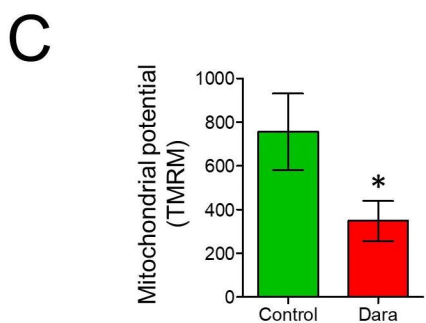
C
Mitochondrial potential
(TMRM)
1000
800
600
400
200
0
*
Control
Dara

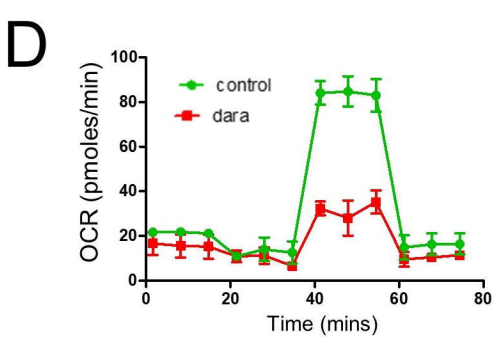
D
OCR (pmoles/min)
100
80
60
40
20
0
control
dara
0
20
40
60
80
Time (mins)

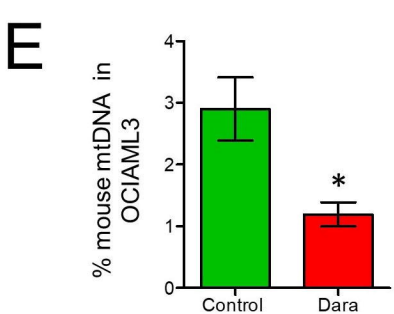
E
% mouse mtDNA in
OCIAML3
4
3
2
1
0
*
Control
Dara